Ride Comfort Analysis of a Vehicle Based on Continuous Wavelet Transform

Sang-Kwon Lee[*†]

Department of Mechanical Engineering, Inha University

Choong-Yul Son

Department of Architecture and Ocean Engineering, Inha University

This paper presents the ride comfort analysis of a vehicle based on wavelet transform. Traditionally, the objective evaluation of impact harshness is based on the vibration dose value (VDV) and frequency weighting method. These methods do not consider the damping effect of the suspension system of a vehicle. In this paper, the damping is estimated using wavelet transform based on Morlet mother wavelet and its effect is considered for the subjective evaluation of impact harshness of a car.

Key Words : Ride Comfort Analysis, Morlet Wavelet, Subjective Evaluation, Suspension

1. Introduction

There is an ongoing demand on manufacturers to produce vehicles with high performance and improved ride comfort (Takata, Ikura and Shimada, 1986; Lee, et al., 1993; Norsworth, 1985) as well as handling and stability. Of particular importance to impact harshness is the ride comfort as a car passes over a rough road. Traditionally, impact harshness has been evaluated subjectively by trained test drivers. The subjective nature of these tests can lead to problems with reproducibility. Thus there is a requirement for objective evaluation. Recently much work has considered the problem of constructing objective measures that correlate well with subjective evaluation (Norsworth, 1985; Varterasian, 1982; Griffin, 1990).

The PSD (Power Spectral Density) is a convenient signal analysis tool and has been applied, in conjunction with a suitable weighting function, as one objective measure (Varterasian, 1982). The PSD is a frequency domain measure; an alternative time domain measure has been suggested by Griffin (Griffin, 1990), namely the VDV (Vibration Dose Value). The VDV consists of the sum of the fourth power of a frequency-weighted acceleration over the period during which the car passes over the rough road. The VDV has been widely used for objective evaluation of ride harshness because it is simple and includes subjective effects. The PSD and VDV express the objective evaluation using the magnitude and exposure time of the vibration signal.

One major factor affecting the impact harshness of a vibration signal is the damping ratio and the damping of a system should also be incorporated into any objective measures. In this paper, the damping ratio is estimated using the continuous wavelet transform. The technique is applied to a Multi-Degree Of Freedom (MDOF) suspension system of a passenger car.

In practical situations, in order to improve impact harshness, the cause of discomfort needs to

† First Author

* Corresponding Author,
E-mail : sangkwon@inha.ac.kr
TEL : +82-32-860-7305; **FAX** : +82-32-868-1716
Department of Mechanical Engineering, Inha University, 253, Yonghywn-dong, Nam-ku, Inchon 402-751, Korea.
(Manuscript **Received** February 21, 2000 ; **Revised** March 2, 2001)

be identified. This paper, first, employs the wavelet transform (Newland, 1994; Kronland and Morlet, 1987; Daubechies, 1992) to identify the cause of discomfort due to impact harshness and also to conduct a modal analysis (Takata, et al., 1986) of the suspension system. Second, both the objective and subjective ratings are evaluated according to the change of the characteristic of the arm bushes of the suspension system. A new method to correlate the objective evaluation with subjective evaluation is developed by establishing a multiple regression model based upon the initial peak values and damping ratios of the vibration data measured under the driver's seat.

2. Wavelet Transform

This section briefly outlines the basics of the wavelet transform. For the spectral analysis of stationary signals, the Fourier transform pair, Eq. (1) are appropriate.

$$X(\omega)=\frac{1}{2\pi}\int_{-\infty}^{\infty}x(t)e^{-j\omega t}dt,\ x(t)=\int_{-\infty}^{\infty}X(\omega)e^{j\omega t}dt \tag{1}$$

However, the Fourier transform of a non-stationary signal fails to clearly present information relating to the temporal variations within the signal. To achieve a representation in which a non-stationary signal is presented in an appropriate manner the time frequency analysis is often used. Such an analysis gives local information pertaining to the spectral content of a signal close to a specific point in time. Some examples of time frequency analysis tools are: the spectrogram, the Wigner-Ville distribution and wavelet analysis. The spectrogram (Koenig, 1946; Lee, 1998b) has limitations because of its poor resolution which is a natural consequence of its use of a windowing function and the uncertainty principle (Cohen, 1995). The Wigner-Ville distribution has a greater capacity for producing high resolution distributions. However, the Wigner-Ville distribution of a multi-component signal contains unwanted interference terms (Wigner, 1932, Lee and White, 1997; Lee and white, 1998a; Lee and White, 1999; Lee, 1999). The wavelet transform is a linear representation and as such does not suffer from interference terms. It is based on the operations of time shifts and frequency scalings (Daubechies, 1992). The wavelet transform trades resolution in a manner that varies over the time-frequency plane, in contrast to the spectrogram in which time-frequency resolution is uniform. In this paper, the wavelet transform is employed for analysis of impact harshness.

2.1 The continuous wavelet transform (CWT)

The CWT is based upon a family of functions,

$$\psi_{a,b}(t)=\frac{1}{\sqrt{a}}\psi\left(\frac{t-b}{a}\right),\ a>b\in\Re \tag{2}$$

where ψ is a fixed function, called the "mother wavelet," that is localised both in time and frequency. The function $\psi_{a,b}(t)$ is obtained by applying the operations of shifting (b- translation) in the time domain and scaling in the frequency domain (a-dilation) to the mother wavelet. The mother wavelet used throughout this paper is the Morlet wavelet (Kronland and Morlet, 1987),

$$\psi(t)=e^{j\omega_0 t}e^{-t^2/2} \tag{3}$$

where ω_0 is the wavelet frequency. The CWT of a signal $x(t)$ is defined by

$$W_x^{\psi}(a,\ b)=\int_{-\infty}^{+\infty}x(t)\psi_{a,b}^{*}(t)dt =\frac{1}{\sqrt{a}}\int_{-\infty}^{+\infty}x(t)\psi^{*}\left(\frac{t-b}{a}\right)dt \tag{4}$$

where $\psi^{*}(\cdot)$ is the complex conjugate of $\psi(\cdot)$ and the function $x(t)$ satisfies the condition,

$$\|x\|^2=\int_{-\infty}^{+\infty}|x(t)|^2dt<+\infty$$

Here $\psi_{a,b}(t)$ plays an analogous role to the $e^{j\omega t}$ in the definition of the Fourier transform. If the mother wavelet, $\psi(t)$, satisfies the admissibility condition:

$$C_{\psi}=\int_{-\infty}^{+\infty}\frac{|\psi(\omega)|^2}{|\omega|}d\omega<+\infty$$

The inverse wavelet transform can be obtained by

$$x(t)=\frac{1}{C_{\psi}}\int_{-\infty}^{+\infty}\int_{-\infty}^{+\infty}W_x^{\psi}(a,\ b)\psi_{a,b}(t)\frac{dbda}{a^2} \tag{5}$$

An alternative formulation of the CWT, (3), can be obtained by expressing $x(t)$ and $\psi(t)$ via their Fourier transforms, $X(a)$ and $\psi(\omega)$, respectively:

$$W_x^{\Psi}(a, b)=\sqrt{a}\int_{-\infty}^{+\infty}X(\omega)\psi^*(a\omega)e^{j\omega b}d\omega$$

The relationship between the scale parameter a and frequency ω can be expressed as (Hlawatsch and Boundreaux, 1991):

$$a=\frac{\omega_0}{\omega} \tag{6}$$

where ω_0 is the frequency of the "mother wavelet," see (3).

2.2 Estimation of damping in the system using the CWT

The impulse response of the linear MDOF system is given by the superposition of N uncoupled single degree of freedom impulse responses, where N is the number of modes. The time frequency analysis decomposes the impulse response into uncoupled impulse responses in the time-frequency plane. The impulse response of the linear MDOF system can be expressed in the following form:

$$x(t)=\sum_{i=1}^{N}X_i e^{-\zeta_i\omega_{ni}t}\sin(\omega_{d_i}t+\theta_i)$$

where X_i is the residue magnitude, ζ_i is the damping ratio, ω_{ni} is the undamped natural frequency, and ω_{d_i} is the damped natural frequency associated with the uncoupled i-th impulse response (*i.e.* i-th mode). An analytic form for the signal, $x(t)$, can be obtained, based on the Hilbert transform and the assumption that the damping ratio is low:

$$\hat{x}(t)=\sum_{i=1}^{N}X_i(t)e^{j\phi_i(t)} \tag{7}$$

where the "hat" notation indicates the analytic form of a signal and $X_i(t)=X_i e^{-\zeta_i\omega_{ni}t}$ and $e^{j\phi_i(t)}=e^{j\omega_{di}t+\theta_i}$. Assuming that the envelope, $X_i(t)$, is slowing varying, then the wavelet transform of $\hat{x}(t)$ can be approximated by substituting (7) into (4) and using (6), one obtains

$$W_x^{\Psi}(t, \omega)=\int_{-\infty}^{+\infty}x(t')\psi_{t,a}^*(t')dt'$$

$$=\sqrt{\frac{\omega}{\omega_0}}\sum_{i=1}^{N}\int_{-\infty}^{+\infty}X_i(t')e^{j\phi(t')}\psi^*\left(\frac{\omega}{\omega_0}(t'-t)\right)dt', \tag{8}$$

Putting $t'-t=\tau$ and assuming that the modulating function $X(t')$ is slowly varying inside the window $\psi(t')$, then one may write $X_i(\tau+t)\approx X_i(t)$. Further expanding $\phi_i(\tau+t)$ into a Taylor series about $t=0$, one obtains

$$W_x^{\Psi}(t, \omega)=\sqrt{\frac{\omega}{\omega_0}}\sum_{i=1}^{N}X_i(t)\int_{-\infty}^{+\infty}e^{j[\phi_i(t)+\dot{\phi}_i(t)\tau+\ddot{\phi}_i(t)\tau^2/2+\cdots]}\psi^*\left(\frac{\omega}{\omega_0}\tau\right)d\tau \tag{9}$$

Neglecting derivatives of $\phi(t)$ of order greater than 1, Eq. (11) can be written as

$$W_x^{\Psi}(t, \omega)=\sqrt{\frac{\omega}{\omega_0}}\sum_{i=1}^{N}X_i(t)e^{j\phi_i(t)}\int_{-\infty}^{+\infty}\psi^*\left(\frac{\omega}{\omega_0}\tau\right)e^{j\dot{\phi}_i(t)\tau}d\tau \tag{10}$$

Identifying the integral in (9) as a Fourier transform and noting that $\dot{\phi}_i(t)=\omega_{d_i}$ allows one to write

$$W_x^{\Psi}(t, \omega)=\sqrt{\frac{\omega_0}{\omega}}\sum_{i=1}^{N}X_i(t)\psi^*\left(\frac{\omega_0}{\omega}\omega_{d_i}\right)e^{j\phi_i(t)} \tag{11}$$

If we use the Morlet wave function, the wavelet transform of $x(t)$ is given by

$$W_x^{\Psi}(t, \omega)=\sqrt{2\pi\frac{\omega_0}{\omega}}\sum_{i=1}^{N}X_i(t)e^{-\frac{1}{2}\omega_0^2\left(\frac{\omega_{d_i}}{\omega}-1\right)^2}e^{j\omega d_i t} \tag{12}$$

Assuming all the damped frequencies, ω_{d_i}, are well separated in frequency, in comparison to ω_0, then the modal contributions in the CWT will be distinct and only the i-th term in the summation in (12) will make a significant contribution. In which case for a fixed value of frequency, $\omega=\omega_{d_i}$, the logarithm of the CWT can be written as

$$ln\,|\,W_x^{\Psi}(t, \omega)\,|\approx-\zeta_i\omega_{in}t+ln\left|X_i\sqrt{2\pi\frac{\omega_0}{\omega_{d_i}}}\right| \tag{13}$$

From which the damping ratio, ζ_i, of the i-th mode of the system can be estimated from the slope of the line obtained by plotting the cross-section $ln\,W_x^{\Psi}(t, \omega_i)$ against time. The successful

Table 1 Comparison between theoretical value and estimated value of damping ratio

	$f_{n_i}=\omega n_i/2\pi$ Undamped Frequency	ζ_i Theoretical damping ratio	ζ_i Estimated damping ratio	% Error
Mode 1	60 Hz	0.01	0.0099	−1
Mode 2	40 Hz	0.2	0.1910	−4.5
Mode 3	40 Hz	0.1	0.0975	−2.5

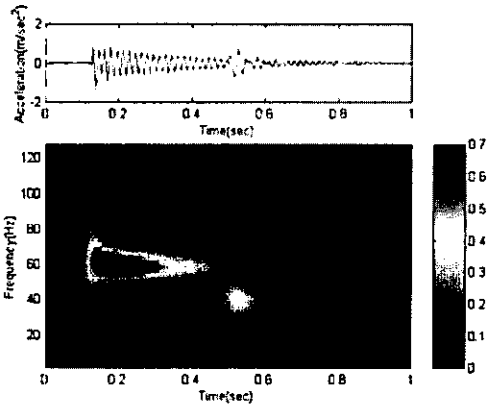

Fig. 1 CWT of the simulated impulse response

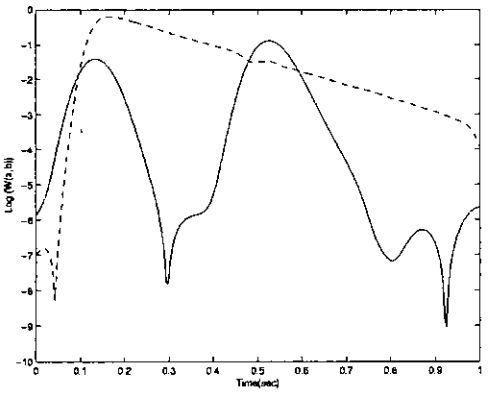

Fig. 2 Cross-section of the CWT for the frequencies; —— : 40 Hz, ····· : 60 Hz

decoupling procedure strictly depends on the separation of modes and wavelet frequency resolution. The wavelet frequency resolution can be controlled by the scaling factor a in Eq. (6). Figures 3(a) and (b) show the octave band frequency resolution of wavelet and the third-octave band frequency resolution respectively. Narrower band frequency resolution also can be made depending on the selection of scaling parameter.

3. Numerical Example

The effectiveness of the procedure for the estimation of damping coefficients, based on the CWT, is demonstrated via a simulation study. The bottom frame in Fig. 1 depicts the CWT calculated from the signal shown in the top frame. The signal represents a synthesised impulse response of a system exhibiting three modes of vibration. The signal is a 256 point time series, sampled at 256 Hz. Each modal contribution is modelled as a damped sinusoid and a low level of Gaussian noise has been added to simulate measurement noise. The first mode is centred in the time-frequency plane at 1/8s and 60 Hz with a damping ratio of 0.01. The second mode is centred in the time-frequency plane at 1/8s and 40 Hz with a damping ratio of 0.2. Finally, the third mode is centred in the time-frequency plane at 1/2s and 40 Hz with a damping ratio of 0.1. In order to estimate the damping ratios of each mode from the impulse response, the cross-section of $ln\,W_x^{\Psi}(t,\ \omega_i)$ is evaluated for the frequencies 40 Hz and 60 Hz; these cross sections are plotted on a logarithmic scale in Fig. 2. Since two of the modes share the same natural frequency (40 Hz), but occur at different times, the corresponding cross-section is more complex than that at 60 Hz in that it contains two peaks. For this curve the two damping ratios are estimated as the slopes of the lines measured directly after the two peaks. For the 60 Hz curve there is only a single response and the slope estimation is correspondingly simpler. The estimated values of damping ratios are listed in Table 1. According to these results, the error increases as damping ratio increases, however the error in each case remains

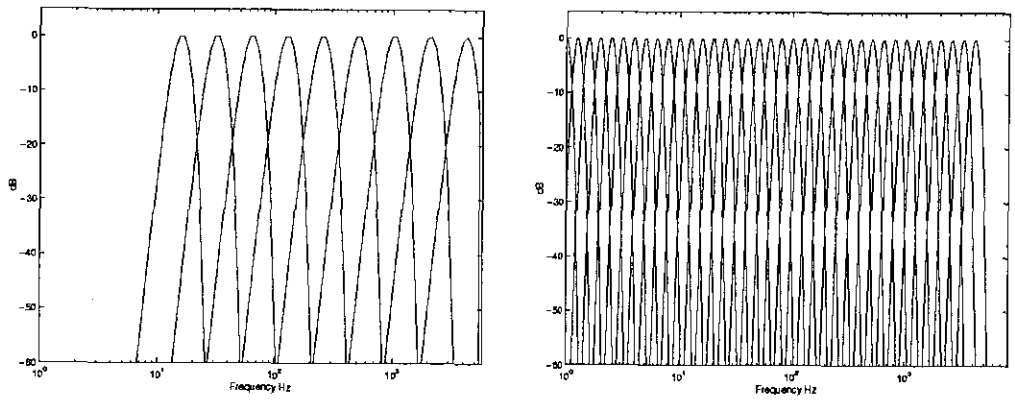

Fig. 3 Wavelet frequency resolution (a) Octave band frequency resolution (b) Third -octave band frequency resolution

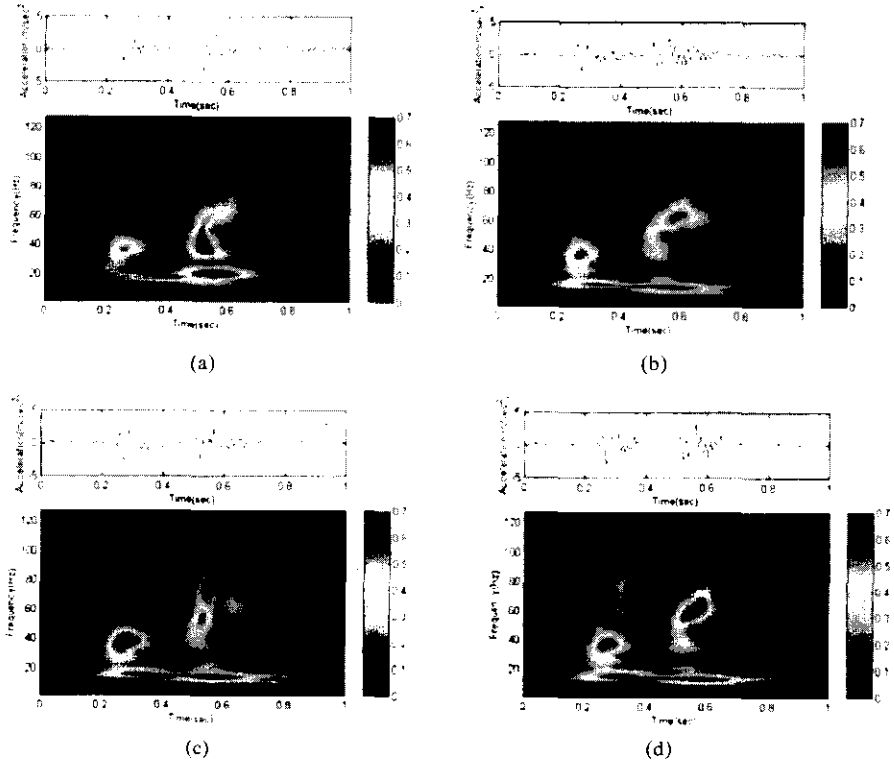

Fig. 4 CWTs of the vibration signals measured using various arm bush stiffness (a) Base (b) 10% down (c) 20% down (d) 30% down

small.

Since each of the modes occupies different regions of the time frequency plane one can apply a mask to the CWT to isolate each mode. Having achieved this the inverse CWT, Eq. (5), can then be applied to construct an estimate of the impulse response of the individual modes (Kronland and Morlet, 1987).

Table 2 Vibration mode of the rear suspension

Frequency (Hz)	Vibration mode
14	Unsprung vertical mode
20	Unsprung longitude mode
40	Suspension & tyre coupling
60	Tyre vertical mode

4. Improvement and Evaluation of Impact Harshness Using Wavelet Transform

To further test this approach, the data from experimental trials were analysed. Figure 4 shows the vibration data measured under driver's seat of a passenger car as it passes over a projection in the road at a speed 40 Km/h. The upper traces in Fig. 4 show the acceleration signal, whilst the lower plots show the CWTs. The four signals in Fig. 4 are generated for different stiffnesses of the arm bushes, with Fig. 4(a) corresponding to the "normal" condition. The car used in these trials had a 2.0 litre gasoline engine. Examination of the time series allows one to see that the response contains two transient components. The first is generated by the impacting of the front wheel on the object in the road and the second arises from the impact of the rear wheel. In this test car, the impact harshness of the rear wheel is a more severe problem than due to the front, according to the subjective evaluation of the test drivers. From the CWT in Fig. 4(a) one can identify three impulsive components corresponding to three modes centred around 20 Hz, 40, and 60 Hz.

In order to further characterise these modes, an experimental modal analysis for the real suspension of the test car is conducted. The model name of test car is SM520 made by Samsung Motor Co. in Korea. Table 2 details the natural frequencies and structures associated with the modes of vibration in the frequency band of interest. The impact harshness problem associated with the test car is a consequence of the impulsive components seen around 40 Hz and 20 Hz near 0. 5s in Fig. 4 (a). They are impact vibrations due to the resonance of the coupled mode of the rear suspension and tyre and an unsprung mass respectively. In order to reduce the impact vibration around 20 Hz and 40 Hz, the unsprung mass is changed and the stiffness of the trailing arm bush is reduced by 10%, 20% and 30%. The results are shown in Fig. 4 (b), (c) and (d) respectively. From the CWTs it can be seen that softening the stiffness of arm bush reduces the impact vibration around 40 Hz, whilst modifying the unsprung mass alters that mode's natural frequency from 20 Hz to 14 Hz. As the stiffness of the arm bush lessens, the component at 40 Hz is reduced, however, the vibration at 60 Hz, that occurs a few milliseconds later, begins to dominate. This 60 Hz component is particularly evident in Figs. 4(b) and (d). By reducing the trailing arm bush stiffness by 20%, both the modes at 40 Hz and 60 Hz are small as seen in Fig. 4(c), but a new component appears at 50 Hz.

In order to understand the effect of these objective observations, a subjective evaluation was also undertaken. The results of subjective evaluation indicate that the 20% stiffness reduction is preferred over the other two reductions. However, it is difficult to correlate the objective results with subjective results directly. Therefore, in order to establish the relationship between the subjective and objective evaluations, three objective rating parameters, namely, the VDV, the initial peak values and the estimated value of damping ratio, are calculated and compared with the subjective rating. The initial peak value is the maximum acceleration measured at the start of the transient signal. The damping ratios are calculated using the CWT computed for cross-sections taken at 40 Hz and 60 Hz. These cross-sections are plotted in Fig. 5 and the estimated damping ratios are listed in the Table 3. From these results, it is found that, the objective parameters computed here, none of them related to the subjective scores in a linear manner. A multiple regression model (Papoulis, 1991; Walpole and Myers, 1993) was employed to fit the initial peak values and damping ratios of vibration modes at 40 Hz and 60 Hz and this was found to be good predictor of the subjective scores. The multiple regression models for the j-th evaluation are given by

Table 3 Comparison of estimated damping coefficients for different suspension systems

	VDV (m/s^2)	ζ_i Estimated damping ratio at 40 Hz	X_i Initial peak values at 0.52sec (m/s^2)	Subjective rating of impact harshness
Base	4.39	0.1619	3.6256	3.5
10%	3.96	0.1462	2.1825	3.0
20%	4.24	0.1659	2.8540	2.0
30%	4.57	0.1128	2.3187	2.5

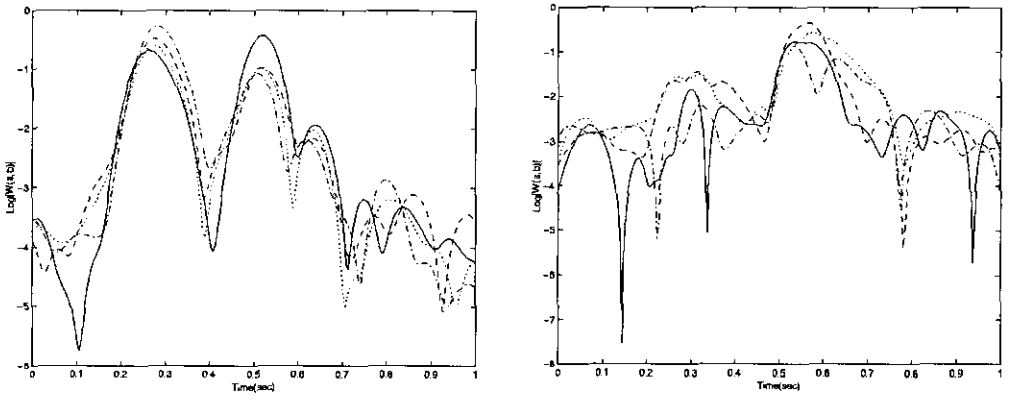

(a) (b)

Fig. 5 Cross-section of the CWT for frequencies around 40Hz and 60Hz; (a) 40Hz (b) 60Hz: base, ·····: 10%, ——: 20%, ------: 30%,-·-·-

$$\hat{y}_{j40}=2.1761-7.1695x_{j1}+0.5922x_{j2} \quad (14)$$

$$\hat{y}_{j60}=4.0388+0.8735x_{j1}-0.4809x_{j2} \quad (15)$$

where $\hat{y}_{j40}$ is the estimated subjective rating (based on objective measurements) using the initial peak value x_{j1} and damping ratio x_{j2} for the vibration mode at 40 Hz and corresponding value for the 60 Hz vibration mode.

To more widely test the validity of the regression model, the objective ratings for 20 trial configurations were estimated using Eqs. (14) and (15). Figures 6(a) and (b) show the comparison between the subjective rating and the rating estimated using objective measures. The regression model is obtained using the least squares method. These trials used 5 sample cars each with the 4 suspension configurations and the average values are shown in Fig. 6. These results demonstrate that the objective evaluation measure developed herein correlates well with subjective evaluation. This allows one to predict the subjective rating for a car based on a few simple parameters; the initial peak value and the damping ratios.

5. Conclusions

The continuous wavelet analysis (CWT) is applied to the objective evaluation of ride comfort of a passenger car. The CWT based on Morlet wavelet is very useful to control the frequency resolution and then to estimate the damping rate relate to the mode of car suspension system. Car suspension system is an important element affect on the ride comfort analysis. The tradition methods for the ride comfort analysis, the spectrum estimation and the vibration dose value, have been used. These methods do not consider the damping effect. In this paper, the damping ratio for vibration modes of suspension system are also considered. The objective evaluation using the CWT based on the Morlet corresponds to the subjective evaluation well for the ride

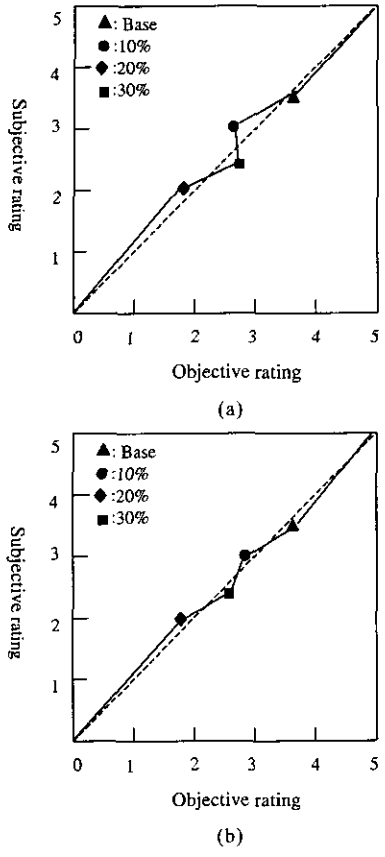

Fig. 6 Comparison between subjective and objective evaluation (a) 40 Hz vibration mode (b) 60 Hz vibration mode

comfort analysis of a passenger car.

Acknowledgments

This work was supported by grant No. 2000-2-30400-004-3 from the Basic research Program of the Korea Science & Engineering Foundation.

References

Cohen, L., 1995, *Time-Frequency Analysis*, pp. 46~49, Prentice Hall.

Daubechies, I., 1992, *Ten Lectures on Wavelets*, Society for Industrial and Applied Mathematics.

Griffin, M. J., 1990, *Handbook of Human Vibration* , Academic Press.

Hlawatsch. F. and Boudreaux, G. F., 1991, "Linear and Quadratic Time-Frequency Signal Representations," *IEEE SP Magazine*, April, pp. 21~67.

Kronland. R. and Morlet, J., 1987, "Analysis of Sound Through Wavelet Transforms," *International Journal of Pattern Recognition and Artificial Intelligence*, Vol. 1, pp. 273~302.

Koenig, R.,1946, "The Sound Spectrogram," *J. Acoust. Soc. Am.*, Vol. 18, pp. 19~46.

Lee, S.K. and White, P. R., 1997, "Fault Diagnosis of Rotating Machinery Using Wigner Higher Order Moment Spectra," *Mechanical Systems and Signal Processing*, Vol. 11, pp. 637~650.

Lee, S. K. and White, P. R., 1998a, "The Enhancement of Impulsive Noise and Vibration Signals for Fault Detection in Rotating and Reciprocating Machinery," *Journal of Sound and Vibration*, Vol. 217, No. 3, pp. 484~505.

Lee, S. K. and White, P. R., 1999, "Two-Stage Adaptive Line Enhancer and Sliced Wigner Trispectrum for the Characterization of Faults from Gear Box Vibration Data," *Transaction of the ASME, Journal of Vibration and Acoustics*, Vol. 121, pp. 488~494.

Lee, S. K., 1998b, "Adaptive Signal Processing and Higher Order Time Frequency Analysis and Their Application to Condition Monitoring," Ph. D. thesis, ISVR, The University of Southampton, U.K.

Lee, S. K., 1999, "Application of the L-Wigner Distribution to the Diagnosis of Local Defects of Gear tooth," *KSME International Journal*, Vol. 13, No. 2, pp. 144~157.

Lee, S.K., Choi, B.U. and Yeo, S.D., 1993, "Identification of Relation Between Crankshaft Bending and Interior Noise of A/T Vehicle in Idle Stage," *The SAE International Congress and Exposition*, Detroit, Michigan, SAE paper No. 930618

Newland, D.E., 1994, *An Introduction to Random Vibration, Spectral and Wavelet Analysis*, 3rd Edition, Longman Scientific & Technical.

Norsworth, T. H., 1985, "The Correlation of Objective Ride Measures to Subjective Jury Evaluation of Class of COE Vehicle," *The SAE International Congress and Exposition*, Detroit,

Michigan, SAE paper No. 850985

Papoulis, A., 1991, *Probability, Random Variables and Stochastic Processes*, 3rd Edition, McGRAW-Hill International Edition.

Takata, N., Ikura, S. and Shimada, T., 1986, "An Analysis of Ride Harshness," *International Journal of Vehicle Design, Special Issue on Vehicle Safety*, pp. 291~303.

Varterasian, J.H., 1982, "On Measuring Automobile Seat Ride Comfort." *The SAE International Congress and Exposition*, Detroit, Michigan, SAE paper No. 820309.

Walpole, R.E. and Myers, R.H., 1993, *Probability and Statistics for Engineers and Scientists*, 3rd Edition, Macmillan Publishing Company.

Wigner, E. 1932, "On the Quantum Correlation for Thermodynamic Equilibrium," *Phys. Rev.*, Vol. 40, pp. 747~759.